Mon. Not. R. Astron. Soc. **000**, 1–12 (2009) Printed 17 August 2009 (MN LaTeX style file v2.2)

arXiv:0908.2434v1 [astro-ph.CO] 17 Aug 2009

Red star-forming and blue passive galaxies in clusters

Smriti Mahajan* and Somak Raychaudhury
School of Physics and Astronomy, College of Engineering and Physical Sciences, University of Birmingham, Birmingham B15 2TT, United Kingdom

ABSTRACT

We explore the relation between colour (measured from photometry) and specific star formation rate (derived from optical spectra obtained by SDSS DR4) of over 6000 galaxies ($M_r \leqslant -20.5$) in and around ($< 3\,r_{200}$) low redshift ($z < 0.12$) Abell clusters. Even though, as expected, most red sequence galaxies have little or no ongoing star formation, and most blue galaxies are currently forming stars, there are significant populations of red star-forming and blue passive galaxies. This paper examines various properties of galaxies belonging to the latter two categories, to understand why they deviate from the norm. These properties include morphological parameters, internal extinction, spectral features such as EW(H$_\delta$) and the 4000 Å break, and metallicity. Our analysis shows that the blue passive galaxies have properties very similar to their star-forming counterparts, except that their large range in H$_\delta$ equivalent width indicates recent truncation of star formation. The red star-forming galaxies fall into two broad categories, one of them being massive galaxies in cluster cores dominated by an old stellar population, but with evidence of current star formation in the core (possibly linked with AGN). For the remaining red star-forming galaxies it is evident from spectral indices, stellar and gas-phase metallicities and mean stellar ages that their colours result from the predominance of a metal-rich stellar population. Only half of the red star-forming galaxies have extinction values consistent with a significant presence of dust. The implication of the properties of these star-forming galaxies on environmental studies, like that of the Butcher-Oemler effect, is discussed.

Key words: Galaxies: clusters: general; galaxies: evolution; galaxies: fundamental parameters; galaxies: starburst; galaxies: stellar content.

1 INTRODUCTION

If, as is widely believed, large-scale structures form in the Universe by means of the hierarchical assembly of dark haloes, one would expect the most massive galaxies to be the youngest, as they would be formed from mergers over time. However, the brightest galaxies, elliptical in morphology, typically found at the centres of rich clusters, appear to be dominated by old stellar populations. Galaxies with current star formation, on the other hand, have been shown to be disc-dominated, mostly occurring in regions of lower density. Such relations between the properties of galaxies and their environment were first pointed out using morphology to characterise galaxies (Oemler 1974; Melnick & Sargent 1977; Dressler 1980), but, in later studies, other photometric properties such as colour (e.g. Kauffmann et al. 2003a; Balogh et al. 2004a; Weinmann et al. 2006; Cooper et al. 2007) have been shown to correlate with environment as well.

In addition to understanding the formation of dark matter haloes, the study of galaxy formation and evolution clearly requires detailed knowledge of the various physical processes that affect baryons, such as mergers, tidal interactions, stripping, cooling and feedback. Observations of the relevant galaxy features and their dependence on environment are very important in our comprehension of the relative importance of these processes, a subject that remains an issue of considerable disagreement (see, e.g., Oemler et al. 2009).

The availability of large-scale spectroscopic surveys, such as the Sloan Digital Sky survey (henceforth SDSS), has resulted in structural parameters of galaxies being largely replaced by spectroscopic properties, in the exploration of the impact of the global and local environment on the nature of a galaxy (Balogh et al. 2004b; Haines et al. 2006a,b; Pimbblet et al. 2006; Porter & Raychaudhury 2005; Weinmann et al. 2006; Porter & Raychaudhury 2007; Porter et al. 2008; Mahajan, Raychaudhury & Pimbblet in preparation, among others). Compared to broad-band colours, spectroscopic parameters such as integrated star formation rate (SFR), specific star formation rate (SSFR or SFR/M*), H$_\delta$ equivalent width (EW) and the 4000 Å break (D$_n$4000), in principle, give more detailed information about the underlying stellar populations in galaxies, but one cannot expect these parameters to behave in the same way with environment as the global photometric properties.

Various factors, including the presence of dust, and the well-known degeneracy between the effect of age and metallicity, pre-

* E-mail: sm@star.sr.bham.ac.uk

vent a straight-forward correspondence between the star formation history of a galaxy and its broad-band colours (e.g., Faber 1973; Calzetti 1997). As a result, the use of broad-band colours and of spectroscopic indicators might yield different classification for a galaxy on an evolutionary sequence. In order to compare observational studies where different photometric or spectroscopic parameters have been used to define sub-samples, one would like to ask, for instance, for what fraction of galaxies the correspondence between morphology, colour and star formation properties fails to hold, and whether such galaxies could be identified from other observable properties. Are these unusual galaxies more likely to occur in certain kinds of environment?

In order to address some of these questions, we choose, for this study, galaxies in and around rich clusters in the low redshift Universe. Galaxy clusters are well suited for such an analysis, since from their cores to their infall regions, they provide a wide range of environments, with varying space density and velocity dispersion. The aim of this work is to examine how well galaxy properties obtained from two mutually independent techniques, namely photometry and spectroscopy, correlate with each other, and to explore the possible causes of discrepancy.

The outline of this paper is as follows: in the next section we define the galaxy sample, and the galaxy properties to be used here. We plot the specific star formation rate of these galaxies against colour, and identify the four classes of galaxies that we will deal with: red sequence, red star-forming, blue star-forming and blue passive. In §3, we examine the various galaxy properties, derived from photometry and spectra, that we use in this analysis. The insight these properties provide into the nature of blue passive and red star-forming galaxies are discussed in §4, and the main conclusions are summarised in §5. Throughout this work we adopt a cosmology with $\Omega_m = 1$ & $\Omega_\Lambda = 0$ and $h = 70$ km s^{-1} Mpc^{-1} for calculating distances and absolute magnitudes. We note that in the redshift range chosen for this work ($0.02 \leqslant z \leqslant 0.12$), the results are insensitive to the choice of cosmology.

2 THE OBSERVATIONAL DATA

We use the spectroscopic galaxy data provided by the SDSS DR4 (Adelman-McCarthy et al. 2006). The SDSS consists of an imaging survey of π steradians, mainly in the northern sky, in five passbands u, g, r, i and z. The imaging is done in drift-scan mode, and the data is processed using the photometric pipeline PHOTO (Lupton et al. 2001) specially written for SDSS. The spectra are obtained using two fibre-fed double spectrographs, covering a wavelength range of 3800-9200 Å. The resolution $\Delta\lambda/\lambda$ varies between 1850 and 2200.

We use the galaxy magnitudes and the corresponding galactic extinction values in the g & r SDSS passbands from the New York University Value added galaxy Catalogue (NYU-VAGC; Blanton et al. 2005). We k-correct these magnitudes to $z = 0.1$ (median redshift of the sample, Yang et al. 2007). We only consider galaxies with absolute magnitude M$_r \leqslant -20.5$ (this corresponds to the apparent magnitude limit for the SDSS spectroscopic catalogue at the median redshift of our sample, $z = 0.1$).

2.1 Cluster membership

We take all Abell clusters (Abell et al. 1989), in the redshift range 0.02$<$ z $\leqslant$0.12, that lie sufficiently away from the survey boundary so as to be sampled out to $\leqslant 6\,h_{70}^{-1}$ Mpc from the cluster centre. We constrain our sample to moderately rich clusters by considering only those that have at least 20 galaxies (brighter than the magnitude limit, M$_r \leqslant -20.5$) with SDSS spectra within $3\,h_{70}^{-1}$ Mpc of the cluster centre. This leaves us with a sample of 119 clusters.

We aim to study the effect of present and recent star formation on the observed properties of galaxies over a wide range of environment, and so we seek to examine galaxies not just in the cores of the clusters, but also on the outskirts. Detailed studies of the velocity structure in the infall regions of clusters show that the turnaround radius of clusters extends out to almost twice the virial radius (Diaferio & Geller 1997; Rines & Diaferio 2006; Dünner et al. 2007), so we chose to examine radial trends of the properties of galaxies out to a projected radius of $R = 6\,h_{70}^{-1}$ Mpc of each cluster centre. Within this radius, we pick galaxies within the following velocity ranges about the mean redshift of the cluster:

$$\Delta z = \left\{ \begin{array}{ll} 3000 \text{ km s}^{-1} & \text{if } R \leqslant 1 \text{ Mpc} \\ 2100 \text{ km s}^{-1} & \text{if } 1 < R \leqslant 3 \text{ Mpc} \\ 1500 \text{ km s}^{-1} & \text{if } 3 < R \leqslant 6 \text{ Mpc} \end{array} \right\}. \quad (1)$$

Adopting these differential velocity slices helps in reducing interlopers, in the absence of a rigorous procedure for assigning cluster membership, and hence is well suited for a statistical study like this. Note that other popular methods, such as the 3-σ_v velocity dispersion cut, are prone to include galaxies at large projected radius from the cluster centre, and our velocity cuts are consistent with the caustics in velocity space used by the CAIRNS survey (e.g. Rines et al. 2003; Rines & Diaferio 2006).

2.2 Cluster parameters

We find the velocity dispersion (σ_v) of each cluster, from the identified members, using the bi-weight statistics (ROSTAT, Beers, Flynn & Gebhardt 1990). The characteristic size of the cluster (the radius at which the mean interior over-density in a sphere of radius r is 200 times the critical density of the Universe) is calculated using the relation given by Carlberg, Yee & Ellingson (1997): $r_{200} = \sqrt{3}\sigma_v/10H(z)$. Our final sample comprises of 119 Abell clusters ($z < 0.12$) in which there are 6,010 galaxies within $3\,r_{200}$ of the cluster centres.

2.3 Galaxy parameters

In this work, we use various quantities derived from the SDSS optical spectra by Brinchmann et al. (2004) (B04 henceforth), based on SDSS DR4 catalogue[1]. From this and related work (Kauffmann et al. 2003b), we use specific spectral indices (emission corrected H$_\delta$ equivalent width and [NeIII] contamination corrected D$_n$4000).

Two of the galaxy parameters we use to begin with, namely the specific star formation rate (SSFR, or SFR/M*) and stellar mass (M*), are derived using the SDSS galaxy spectra by B04 and Kauffmann et al. (2003b) respectively. B04 construct a grid of $\sim 2 \times 10^5$ spectral synthesis models (Bruzual & Charlot 1993; Charlot & Longhetti 2001) over four relevant parameters spanning a range in metallicity (Z) of $-1 < \log Z/Z_\odot < 0.6$, ionization parameter ($U$) $-4.0 < \log U < -2.0$, total dust attenuation (τ_V) $0.01 < \tau_V < 4.0$ and dust-to-metal-ratio (ξ) $0.1 < \xi < 0.5$. The attenuation by dust is treated using a physically motivated model

---

[1] http://www.mpa-garching.mpg.de/SDSS/DR4/Data/sfr_catalogue.html

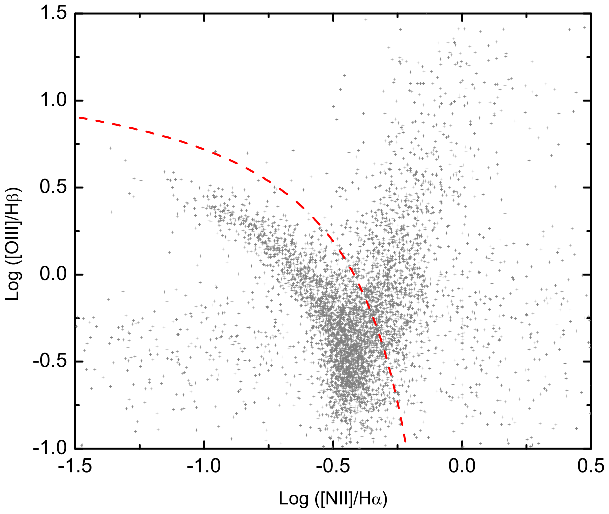

Figure 1. The distribution of the galaxies used in this work in the plot of the two line-ratios, recommended by Baldwin, Phillips & Terlevich (1981, (BPT)), that are often used to discriminate between star-forming (and composite) galaxies (below the *red* line; Kauffmann et al. (2003c)) and the AGN-dominated galaxies (above). All galaxies in our sample, except the 'unclassified', are plotted here.

of Charlot & Fall (2000), which provides a consistent model for ultra-violet (UV) to infra-red (IR) emission.

B04 compare the modelled line-ratios for each model in their grid directly with those in the observed spectrum, and, for each galaxy, construct a log-likelihood function for each point on the model grid, summed over all lines observed in the spectrum of that galaxy. It is worth mentioning here that since they study relative line fluxes only, their analysis is insensitive to stellar ages, star formation history and the relative attenuation by dust in the molecular gas clouds and the interstellar medium.

B04 derive their values for star formation rate (SFR) and specific star formation rate (SFR/M*) using a Bayesian technique, involving the likelihood functions mentioned above, using the entire spectrum of each galaxy (it is worth noting that the spectrum comes from a fibre of diameter $3''$). It is shown that their work yield better estimates of the SFR and SFR/M* than any single spectroscopic SFR indicator, such as equivalent width (EW) of the H$_\alpha$ or O II lines, which are used extensively in the literature. Furthermore, the combination of several line indices enables one to separate the galaxies with a significant AGN component from those with emission entirely due to star formation. The derived parameters (SFR and SFR/M*) are then corrected for aperture biases using their photometric colours. Out of the three statistical estimates (mean, median and mode) for the probability distribution function (PDF) of SFR and SFR/M* derived for each galaxy, we use the median of the distribution in this work for each quantity, since it is independent of binning.

Star-forming galaxies can be separated from the AGN-dominated ones on the basis of the so-called BPT diagram (Baldwin, Phillips & Terlevich 1981), namely a plot of the line ratio [OIII]/H$_\beta$ against H$_\alpha$/[NII], Fig. 1, for galaxies with all four emission lines. B04 divide all galaxies into four classes (star forming, AGN, composite and unclassified) using the BPT diagram. For those galaxies whose spectra do not show all the above mentioned emission lines, (called 'unclassified' galaxies), and those that are classified as AGN-dominated, B04 adopt an indirect method for estimating the SFRs. They use the relationship between the D$_n$4000 and SFR derived for the high S/N ($\geqslant$ 3) star-forming galaxies (SFR$_e$) to estimate the SFR of the AGNs and low S/N galaxies (SFR$_d$; see section 4.1 of B04 for details). Using the entire spectrum also makes it possible to obtain an independent estimate of stellar mass M*, which further constraints the estimated SFR/M*, making it a more reliable parameter for evaluating star formation properties of galaxies, compared to other luminosity based parameters employed elsewhere (e.g. Lewis et al. 2002; Gòmez et al. 2003). Kauffmann et al. (2003a) adopt similar methodology as B04 for estimating the stellar mass M*. Their models are characterised by star-to-light ratio, dust attenuation and fraction of mass formed in a major burst of star formation (the burst mass fraction). They then compute the total mass in stars by multiplying the dust-corrected and k-corrected z-band luminosity of the galaxy, by the estimated z-band mass-to-light ratio of the best-fitting model, found using the Bayesian technique described above.

Several authors have shown that the SFR of a galaxy scales with its stellar mass (e.g. Noeske et al. 2007). Since the reason for this correlation is yet unclear, and beyond the scope of this work, we employ the specific star formation rate SFR/M* as the more reliable measure of the star formation activity of galaxies. The values of SFR (and SFR/M*) derived for the galaxies with emission lines, i.e. all but those categorised as 'unclassified', are reliable (see Fig. 14; B04), because the classification requires S/N>3 in all the 4 lines involved in the BPT diagram (i.e., H$_\alpha$, H$_\beta$, [OIII] and [NII]). But for spectra of galaxies without emission lines, or of those that are unclassified (most of which are passive), the uncertainties are relatively higher. We chose not to select galaxies based on the confidence interval values derived from the PDF of the SFR and SFR/M* parameters of individual galaxies, because excluding galaxies with higher uncertainties in SFR/M* (or SFR) distribution would preferentially exclude a significant number of passive galaxies and thus bias our samples.

2.4 Four categories of galaxies

Galaxy properties measurable from photometry or spectra, such as colour, SFR or SSFR (SFR/M*) have been extensively used in studies of their dependence on the environment of the galaxy (e.g. Balogh et al. 2004b; Haines et al. 2006a,b; Pimbblet et al. 2006; Weinmann et al. 2006; Porter & Raychaudhury 2007; Porter et al. 2008; Mahajan, Raychaudhury & Pimbblet in preparation), or on other variables representing mass, such as the stellar mass of the galaxy (Kauffmann et al. 2003b) or its circular velocity (Graves et al. 2007).

In this work, we study the colour and SSFR as indicators of the evolutionary stage of a galaxy. In Fig. 2 we plot the colours of all galaxies found within $3\,r_{200}$ of the centres of all the clusters in our sample against their specific star formation rates. In a pioneering study of evolution of galaxies in clusters, Butcher & Oemler (1984) had adopted a colour cut to define blue galaxies as $B-V=0.2$ mag lower than the cluster's red sequence. Here we stack all the cluster galaxies together, and fit a red sequence to galaxies which has a slope of -0.034 with an absolute deviation of 0.080. Since this slope is negligible, we adopt a null slope red sequence at $(g-r)^{0.1}=1$. We note that using the actual red sequence fit does not change our results at all. The blue galaxies are thus defined to have $(g-r)^{0.1}\leqslant 0.8$. This classifies $\sim$25% of all galaxies as blue.

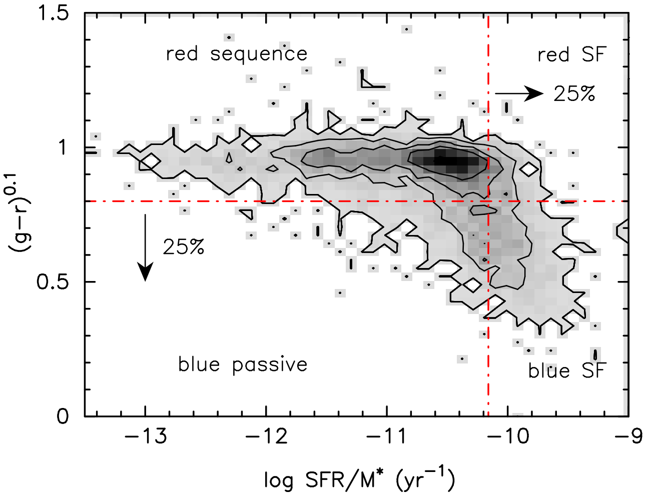

Figure 2. The relation between specific star formation rate (SSFR or SFR/M_*) for all galaxies found within $3\,r_{200}$ of the centre of each galaxy cluster in our sample. The contours represent 150, 100, 50 and 25 galaxies respectively. The horizontal line marks the colour cut adopted by most Butcher-Oemler effect studies, i.e. 0.2 mag bluer than the red sequence: this labels $\sim$ 25% of all galaxies as blue. To match this cut, we adopt a SSFR threshold, log SFR/M*$=\,-10.16$ yr^{-1} such that 25% of all the galaxies are classified as star-forming. We thus categorise our galaxy ensemble into four classes: (*clockwise from right*) red star-forming, blue star-forming, blue passive and red sequence galaxies respectively.

Table 1. Number of galaxies in the four categories

	red SF	red sequence	blue passive	blue SF
Clusters	539	3998	538	935
Entire SDSS	24039	163904	44877	113909

Correspondingly, we choose the SSFR threshold at log SFR/M*= -10.16 yr^{-1}, defining the 25% of all galaxies with a higher value of SSFR as star-forming. We note that our results do not qualitatively change even if the SSFR threshold is changed to the 50-percentile value (log SFR/M*= -10.45 yr^{-1}). We thus classify the galaxies in the 4 quadrants of Fig. 2 as red star-forming, red sequence, blue passive and blue star-forming, anti-clockwise from top right. Table 1 gives the number of galaxies in our cluster sample in each category, and also the corresponding numbers in the whole of SDSS DR4 spectroscopic catalogue in the same redshift and magnitude range as our cluster galaxy sample.

2.5 Spatial distribution of galaxies in clusters

Having divided the galaxies into four classes, we consider their radial distribution within the clusters to examine the possible influence of local environment. Fig. 3 shows the distribution of galaxies in all four categories as a function of distance from the corresponding cluster, scaled by r_{200}. For each category, the curve has been normalized by the total number of galaxies in that category.

As expected, the fraction of the passive red sequence galaxies increase towards the cluster centre. The red star-forming galaxies closely follow the distribution, but their fraction inside r$_{200}$ does not increase as steeply as that of the red sequence galaxies, suggesting a different evolutionary path. Here it would have been very interesting to examine the detailed difference between these two distributions as a function of halo mass, since in both clusters and groups the morphology and star formation properties seem to vary between dwarfs and giants (Khosroshahi et al. 2004; Miles, Raychaudhury, & Russell 2006), and/or central and satellite galaxies (Ann, Park, & Choi 2008), indicating different evolutionary histories. But in this work, over the redshift range of our sample, we have to be confined mostly to M_* and brighter galaxies ($M_r \leqslant -20.5$).

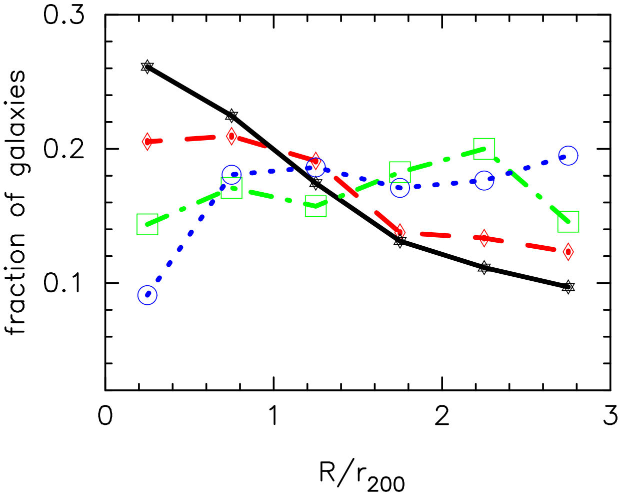

Figure 3. The radial distribution of galaxies in the four categories defined in §2.4 is plotted as a function of cluster-centric radius, scaled by r_{200}. Each distribution is normalized to unity. The Poisson error on each point is smaller than the size of symbols. The fraction of red sequence galaxies *(black)*, as expected, increases toward the cluster centre, and the red star-forming galaxies *(red)* follow them closely. The blue star-forming galaxies *(blue)* show a decline within r_{200}, while their passive counterparts *(green)* show a constant fraction out to $3\,r_{200}$, except for a mild increase $\sim 2r_{\,200}$.

At the other extreme, the blue star-forming galaxies show a constant distribution beyond r$_{200}$, dropping steeply in the cluster core. This is the consequence of the observed lack of neutral gas in galaxies in the cores of rich clusters (e.g. Giovanelli & Haynes 1985; Raychaudhury et al. 1997).

However, the blue passive galaxies, which also have a more or less constant radial distribution over the entire range, do not show this rapid drop in the cores. This is consistent with the observation, discussed below in some detail, of nuclear star formation in a substantial fraction of brightest cluster galaxies (Bildfell et al. 2008; Reichard et al. 2009), which will cause the innermost bin to be significantly higher for this distribution than that for the blue star-forming galaxies. It is interesting to note that the fraction of blue passive galaxies also show a minor increment around 2r$_{200}$. Other studies have shown that in clusters, particularly those that are fed by filaments, there is an enhancement of nuclear star formation in the infalling galaxies beyond r$_{200}$ (e.g. Porter & Raychaudhury 2007; Porter et al. 2008; Mahajan, Raychaudhury & Pimbblet in preparation).

3 DO THE GALAXY PROPERTIES DERIVED FROM PHOTOMETRY AND SPECTROSCOPY AGREE WITH EACH OTHER?

One of the objectives in this paper will be to examine the hypothesis that the galaxy populations can indeed be divided, on the basis of a single parameter, into two classes: passive and star-forming, and that the incidence of red star-forming or blue passive galaxies is merely due to the scatter in the measured parameters within reasonable errors. As we show below, this hypothesis fails to hold.

3.1 The effect of extinction and abundance

Star-forming regions in a galaxy are often surrounded by dust, which can significantly affect quantitative analyses based on optical light. Conversely, the presence of dust in a galaxy would imply the presence of star-forming regions therein. In the absence of infrared observations, which are often used to quantify the effect of dust in star-forming systems (e.g. Calzetti 1997), optical photometry can also be used to constrain the internal extinction in a galaxy (also see Fig. 9).

In one such attempt, Kauffmann et al. (2003b) have estimated the degree of dust attenuation in the SDSS z-band, by comparing model colours to the measured colours to estimate the reddening for each galaxy. The shape of the attenuation curve from observations is found to resemble a power law with slope ~ -0.7 over a wavelength range from 1250-8000 Å (Calzetti et al. 1994). A standard attenuation curve, of the form $\tau_\lambda \propto \lambda^{-0.7}$, is then extrapolated to obtain the extinction in the SDSS z-band. We use the A_z values from Kauffmann et al. (2003b), expressed in magnitudes, in this section. The typical 1σ error on the estimated A_z is ~ 0.12 mag. They also note that comparison of $g-r$ and $r-i$ colours yield similar extinction values for most galaxies if the colours are corrected for nebular emission.

The reddening of a galaxy is the result of a combination of several factors, involving the presence of dust and/or metals in the interstellar medium and of old stars. In our attempt to interpret the apparent evidence of star formation in the fibre spectra of some red galaxies (‘red SF’), and the low values of SFR in the spectra of some blue galaxies (‘blue passive’), we plot, in Fig. 4, the distribution of internal extinction A_z of the galaxies in the four populations as classified in Fig. 2.

As expected, the ‘red sequence’ galaxies, most of which are passively evolving massive galaxies in the cores of clusters, show very little extinction (negative values of A_z being interpreted as zero here). However, even among passive galaxies, there is a small fraction that constitutes a tail extending to non-negligible extinction values. The blue star-forming galaxies, on the other hand, show a clear sign of attenuation going upto 1.9 mag in the z-band, with most galaxies having extinction values around 0.6 mag for the blue star-forming galaxies and 0.35 mag for the blue passive galaxies respectively.

In contrast, the red star-forming galaxies show a mix of at least two different populations: about half of them are unattenuated (similar to the red sequence galaxies), and the other half contributing to the skewed high extinction end of the distribution. We employ the KMM algorithm (Ashman, Bird & Zepf 1994) to quantify the existence of bimodality in our data. The KMM algorithm fits a user specified number of Gaussian distributions to the dataset, calculates the maximum likelihood estimate of their means and variances, and assesses the improvement of the fit over that provided by a single Gaussian. The KMM likelihood ratio test statistics (LRTS) used here is a measure of improvement in using two Gaussian distributions (since we are testing bimodality) over a 1-mode fit.

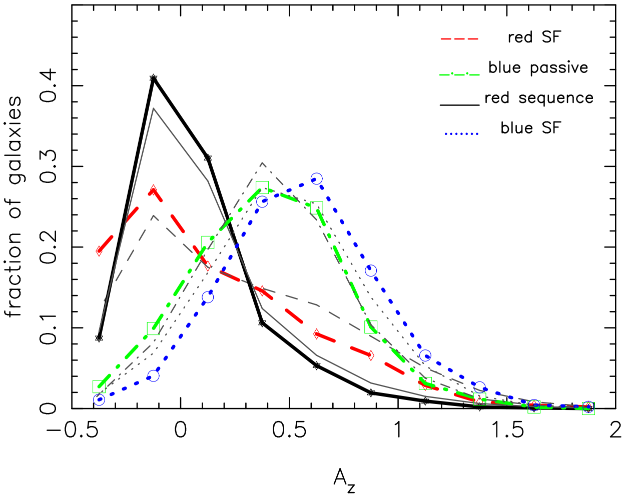

Figure 4. The distribution of internal extinction among our cluster galaxies in the four quadrants as specified in Fig. 2. Each histogram is normalized to unity. It is clear that in general more ‘blue’ galaxies are prone to internal reddening than the ‘red’ ones, with star-forming (*blue dotted*) and passive blue galaxies (*green dot-dashed*) showing slight offsets. Interestingly, while < 45% of the red sequence galaxies (*black solid*) show signs of some extinction, the red star-forming galaxies (*red dashed*) have a bimodal distribution in extinction values (see text). The *grey lines* represent the same distributions as above, but for $> 300,000$ galaxies found in the entire SDSS DR4, divided in the four quadrants in the same way as described for the sample of cluster galaxies studied here. Here, negative values of A_z indicate the absence of extinction.

For the distribution of extinction, in the red star-forming galaxies the KMM test gives the value of likelihood ratio (LRTS) to be 75, when using a bimodal fit to the data than using a unimodal fit, with nil probability of the null hypothesis being satisfied. The 2-modes of the internal extinction distribution are found to be centred around A$_z$=-0.06 (read zero extinction) and 0.72 mag respectively for the sample of cluster galaxies. Interestingly, we find that even by changing the selection criteria for defining the red star-forming galaxies to a higher value of log SFR/M* = -10 yr^{-1}, the KMM test still yields statistically significant result in favour of a bimodal fit to the data (LRTS=21 at a significance level 5×10^{-5}).

Along with the distribution of extinction values for the cluster galaxies, we also show the corresponding distributions for $>$300,000 galaxies, with the same magnitude and redshift range as our cluster sample, drawn from the entire SDSS DR4 spectroscopic catalogue (grey thin lines). For this much larger sample, the histograms of extinction values are not significantly different from those for the cluster sample, except for the red star-forming galaxies, where cluster galaxies seem to have relatively fewer galaxies with high extinction values than similar galaxies in the larger all-SDSS sample.

3.2 H$_\delta$ and the 4000Å break

In order to probe the presence of young (< 1 Gyr old) stellar populations among galaxies with an unusual combination of SFR/M* and colour, we plot the distributions of the EW of the H$_\delta$ absorption line, and of the D$_n$4000 values in Figs. 5 and 6 respectively. The D$_n$4000 is the strongest discontinuity occurring in the optical spectrum of a galaxy, mainly due to the presence of ionised metals. On the other hand, H$_\delta$ absorption is detected after most of the massive hot stars have finished evolving on the main sequence, i.e. at least 0.1-1 Gyr after a starburst is truncated. Thus the H$_\delta$ EW is a measure of the age of the youngest stellar population in a galaxy, and has been extensively used to estimate the mean stellar ages as well (Worthey & Ottaviani 1997). Even though several studies have shown that the Balmer emission due to HII regions, AGN

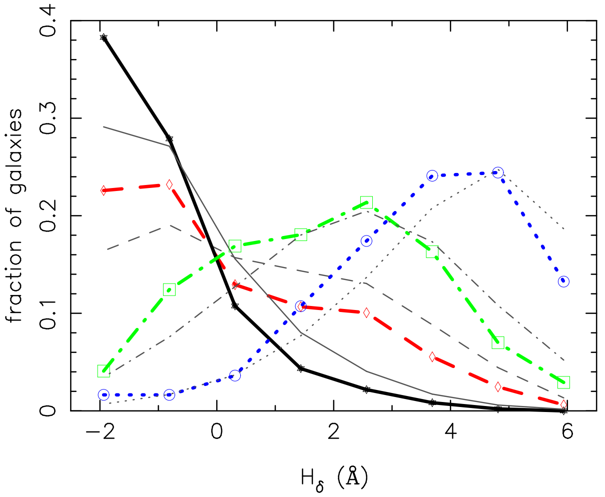

Figure 5. The distribution of the (emission corrected) H_δ equivalent width (EW) for galaxies in our cluster sample, with line styles the same as in Fig. 4. As expected, the blue star-forming galaxies have the highest absorption, showing the presence of $<$ 1 Gyr old stellar population/s, while the red sequence galaxies show little evidence for absorption in H_δ. The blue passive galaxies have a broad distribution with equal probability of finding H_δ in emission (negative EW) or absorption. The distribution for red star-forming galaxies is bimodal, which, in conjunction with the distribution of their internal extinction (Fig. 4), indicates the presence of two distinct galaxy populations.

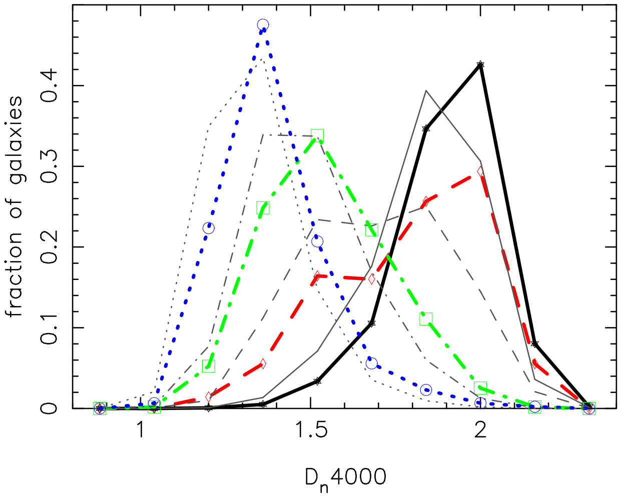

Figure 6. The distribution of the (NeIII continuum corrected) D_n4000 values, with line styles the same as in Fig. 4. As expected, the red sequence galaxies have the largest values, while the blue star-forming galaxies the smallest values for D_n4000 respectively. The blue passive galaxies have a small offset ($\sim$ 0.2) from their star-forming counterparts, revealing the presence of slightly older stellar populations. The histogram for red star-forming galaxies has a statistically significant bimodality (see text), similar to that seen in Figs. 4 & 5.

and/or planetary nebulae can fill in the underlying Balmer absorption lines, causing age estimates to be spuriously high (Trager et al. 2000; Prochaska et al. 2007), the H_δ EW remains a popular stellar age indicator because it is less affected than the lower order Balmer lines, due to the steep Balmer decrement in emission (Osterbrock 1989; Worthey & Ottaviani 1997).

Here we use the measured values of the (emission corrected) H_δ EW, and the (NeIII continuum corrected) D_n4000 from Kauffmann et al. (2003b), who, for the latter, have adopted a modified version of the original definition (Bruzual 1983) of the D_n4000 introduced by Balogh et al. (1999). A stronger D_n4000 is an indicator of a metal-rich inter-stellar medium, which, together with the H_δ EW, indicates whether the galaxy has been forming stars continuously (intermediate/high D_n4000 plus low H_δ EW) or in bursts (low D_n4000 plus high H_δ EW) over the past 1-2 Gyr (Kauffmann et al. 2003b). We note that the observational error in D_n4000 index is very small, typically $\sim$0.02, but the same is not true for the H_δ EW, which has an uncertainty of 1-2 Å in measurement (Kauffmann et al. 2003b). Kauffmann et al. (2003b) discuss the physical constraints leading to these uncertainties, and show that the H_δ index can assume only a selected range of values for all possible star formation histories. The large observational errors on the H_δ EW imply that the estimated value of this index is constrained by the parameter space spanned by the acceptable models.

The red sequence galaxies in our sample show H_δ in emission, and yield large values for the D_n4000, confirming the fact that their main ingredient is a population of old, passively evolving stars, which determines the overall galaxy colours and dominates the spectra. The high observational uncertainty in the EW(H_δ) implies that it is hard to determine whether H_δ is actually occurring in emission, or the negative EWs are a result of a high correction factor in individual galaxies. This is a common problem with the use of H_δ index in individual systems, but this might not be an important issue for this statistical study. The blue star-forming galaxies, in sharp contrast, yield small values for the D_n4000 and strong H_δ in absorption. The blue passive galaxies follow the blue star-forming galaxies, with the mean value for the D_n4000 systematically higher by $\sim$ 0.2, but with a very broad distribution of H_δ EW, revealing a mix of galaxies with a large scatter in the ages of their youngest stellar populations. In red star-forming galaxies, the distributions of H_δ EW as well as the D_n4000 are bimodal. The KMM test prefers a 2-mode fit over a 1-mode fit with likelihood ratios of 78 and 84, for H_δ EW and D_n4000 respectively, with zero probability for the null hypothesis in both cases.

We also check whether this bimodality is a result of the threshold chosen to define whether a galaxy is star-forming or not. As for the internal extinction, the KMM test results remain statistically significant, for both H_δ EW and the D_n4000, when the red star-forming galaxies are selected with an even higher SSFR threshold (log SFR/M* = –10 yr^{-1}), showing that these results are not sensitive to how the four categories are chosen, within reasonable limits. The above results become even more convincing when we plot the four different galaxy populations on the plane defined by the two indices D_n4000 and EW(H_δ) (Fig. 7). Kauffmann et al. (2003a) have shown that these two indices taken together can very effectively determine the star formation history of a galaxy. As shown in Fig. 7, this indeed seem to be the case. The blue star-forming and the passive, red sequence galaxies occupy the opposite ends of the space. But whilst the blue passive galaxies seem to follow the blue star-forming galaxies, although with somewhat lower EW(H_δ) and higher D_n4000, the red star-forming galaxies span the entire range of values in both indices, as would be expected given their bimodal distribution.

3.3 AGN and star formation

Figs. 4, 5, 6 and 7 clearly show that while most of the cluster galaxies follow the classical picture, blue colours correlating with higher SSFR, and redder colours with negligible star formation activity, there is a non-negligible fraction of galaxies in either class which

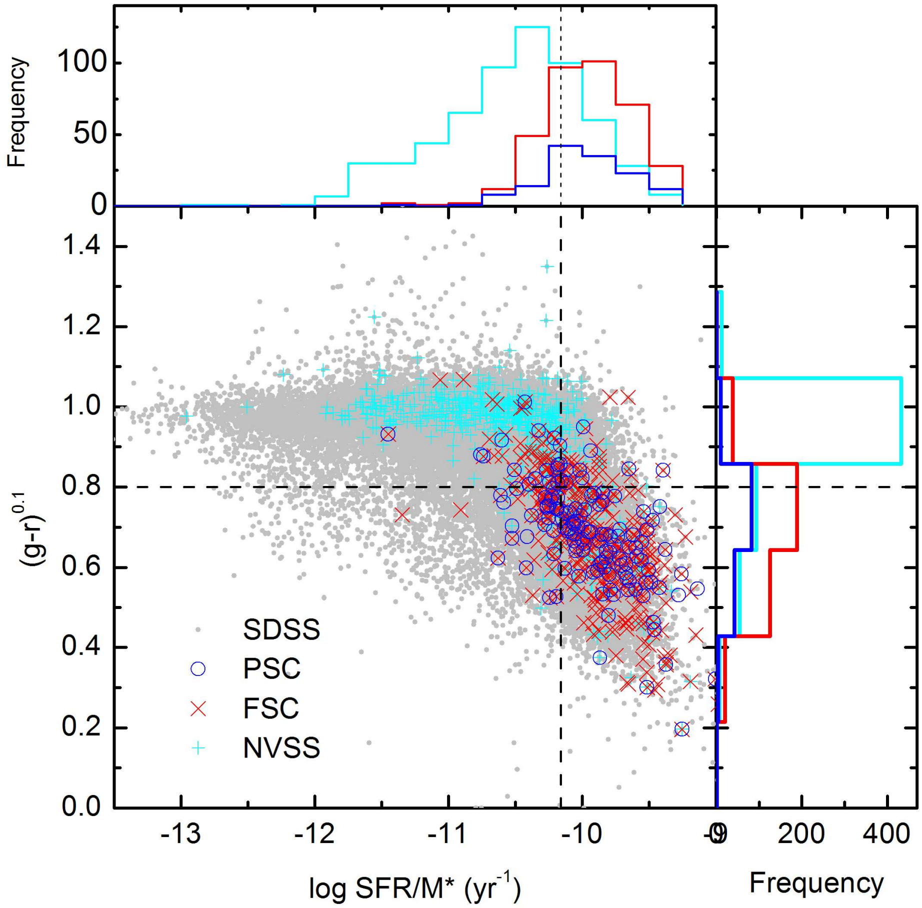

Figure 9. The central panel of this plot shows the $(g-r)^{0.1}$ colour of all the spectroscopically covered SDSS DR4 galaxies (*grey dots*) in the colour-SSFR space (same as Fig. 2), found in the same redshift range and magnitude limit as our cluster galaxy sample. Over-plotted are 1.4 GHz radio sources from the NVSS (*cyan*), *IRAS* point sources (PSC, *blue*) and IRAS faint sources (FSC, *red*) respectively. The top and the right panel show the histograms of these quantities along the two axes. As expected, most of the radio-loud AGN concentrated along the red sequence, and IR bright sources in the blue star-forming galaxies. It is interesting to note that the red star-forming galaxies (top right quadrant, central panel), a large fraction of which are expected to be dust-reddened, do not seem to have many IRAS sources. This supports our conclusion here that a non-negligible fraction of the red star-forming galaxies obtain their colour from the presence of excessive metals.

deviate from the norm. It is thus crucial to understand the properties of these galaxies and identify the cause of their occurrence. In order to do so, we make use of the classification of galaxies, based on the BPT diagram, as star-forming, composite, AGN and those without emission lines (unclassified), as mentioned above in §2.3.

Ignoring, for the time being, the unclassified galaxies for which the nature of star formation activity cannot be conclusively determined from the spectroscopic data, we find that >30% of the red star-forming galaxies and ∼50% of the red sequence galaxies are classified as AGN. This agrees with the well-known observation that AGN are predominantly hosted by the massive elliptical galaxies. In Fig. 9, we plot 1.4GHz radio sources (from NVSS, Best et al. 2005) and IRAS 60μm sources found in the SDSS DR2 (Cao et al. 2006), along with all the galaxies found in the same redshift range ($z \leqslant 0.12$) and magnitude limit ($M_r \leqslant -20.5$) in our galaxy sample. The radio-loud AGN are clearly seen to be hosted mostly in the red sequence galaxies. Interestingly, not many of the red star-forming galaxies are found in the IRAS 60μm source catalogues, disagreeing with the usual expectation that the colour of the red star-forming galaxies is a result of the presence of dust around star-forming gas clouds. We further explore this issue in §4.2.

3.4 Aperture vs global colours

An SDSS spectrum comes from a fixed aperture, which is equal to the diameter of the fibres ($3''$) used in the spectrograph. Since this aperture would encompass a varying fraction of the light of a galaxy depending upon its size and distance, going up to ∼40-60% at $z = 0.1$, the spectrum might not, in most cases, be a true representation of the galaxy's mean overall star formation activity. In this work, we compare photometric colours and spectroscopically derived specific star formation rates, which come from independent observations of the same galaxies. It would be interesting to see how the colour derived from the fibre aperture, as opposed to

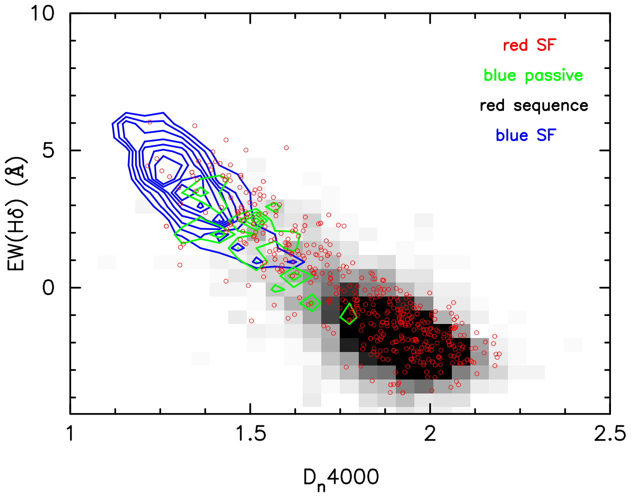

Figure 7. The relation between the equivalent width of the H_δ line EW(H$_\delta$) and the 4000Å break index D$_n$4000, for all galaxies in our sample. These two indices together form a robust diagnostic of the star formation history of a galaxy, irrespective of the stellar ages and metallicity (Kauffmann et al. 2003a, also see text). The red sequence galaxies *(grey scale)* form a core in the passive region of the plane, while the blue star-forming galaxies *(blue contours)* occupy the region indicating recent and ongoing star formation. The blue passive galaxies *(green contours)* closely follow the blue star forming galaxies, but with somewhat higher D$_n$4000 and low EW(H$_\delta$), indicating recent truncation of star formation. The innermost contours represent 24 galaxies in both cases, and the number decreases by 3 at every successive level of contour. The red star-forming galaxies seem to span the entire range in both indices defining this space, a relatively large fraction of them being passively evolving just like the red sequence galaxies, but a non-negligible fraction intruding the space dominated by the blue star-forming galaxies.

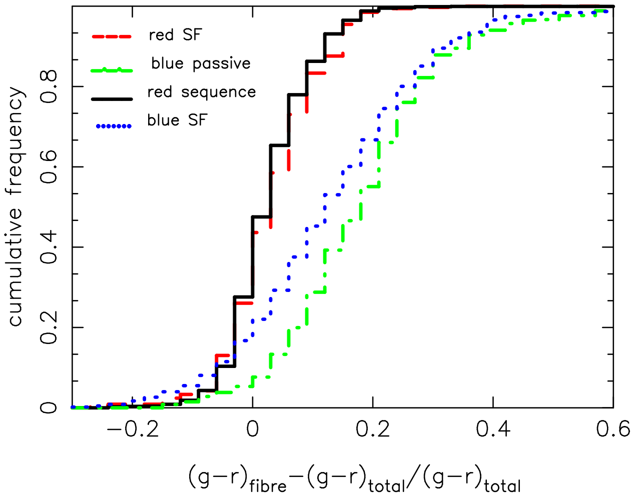

Figure 8. The cumulative distributions of $g-r$ aperture colour, measured within the $3''$ SDSS fibre, relative to the overall colour of the entire galaxy. At $z\sim0.1$, $>60\%$ of the light in the fibre comes from the bulge and hence the fibre colour can be assumed to be a proxy for the colour of the bulge. The slope of the distributions for blue galaxies is much steeper than that of the red ones, showing the large spread in the relative colour, irrespective of the SSFR. Although the red galaxies have a relatively small spread in colour, a significant number of red star-forming galaxies have bluer bulges. This could be the signature of the presence of active nuclei supporting star-formation activity in the core of the galaxies, while the overall galaxy colour remains dominated by the older stellar population elsewhere in the galaxy.

the value averaged over the entire galaxy, relates to SSFR. For instance, if an early-type galaxy has significant star formation in the core, we would expect to see a bluer core, while the overall photometric colour would be dominated by the older stellar populations elsewhere in the galaxy.

In Fig 8, we plot the difference between the colour measured within the fibre and the overall colour of the galaxy, normalised by the overall colour, separately for galaxies belonging to the four categories. A noticeable characteristic of this plot is that irrespective of their star formation properties, the blue and red galaxies have very different slopes for this cumulative distribution. The steeper slope for the blue galaxies is a consequence of their wider range in colour. While most of the galaxies have fibre colours that are redder than the overall galaxy colours, $\sim$15% of the blue star-forming and $\sim$15% of the red star-forming and red sequence galaxies have bluer cores. This suggests the presence of centrally concentrated star formation in these galaxies. It must be noted that although relative fibre colour is a good first approximation to the colour of the bulge of a galaxy, in this work where we stack galaxies over a range of redshift, the ratio of central and overall colour is not derived on the same physical scale for all galaxies. This result should therefore be considered to be a qualitative one.

4 DISCUSSION

Numerous studies of the evolution of galaxies have made use of either global photometric properties such as colour (e.g. Butcher & Oemler 1984), morphology (Dressler 1980) or luminosity of a galaxy, or spectroscopic properties such as circular velocity (e.g. Graves et al. 2007), the D$_n$4000, EW of H$_\delta$ absorption line (e.g. Balogh et al. 1999), emission lines of H$_\alpha$ or OII (e.g. Lewis et al. 2002; Gòmez et al. 2003; Balogh et al. 2004b; Haines et al. 2007) or integrated SFR and/or SSFR (B04). Often samples are chosen based on colour or star formation properties. Are the properties derived from photometry and from spectra correlated enough to yield similar results?

Blue galaxies are thought to be of late-type morphology and and have significant star formation activity, while red galaxies are early-type and show little or no evidence of current star formation. However, with the recent availability of extensive multi-wavelength photometric databases, and of large optical spectroscopic surveys, several authors (e.g. Wolf, Gray & Meisenheimer 2005; Bildfell et al. 2008; Haines et al. 2008; Koyama et al. 2008; Saintonge, Tran & Holden 2008; Graves, Faber, & Schiavon 2009; Wolf et al. 2009) have suggested that optical colour may not necessarily be a good representation of a galaxy's evolutionary state. In this paper, we have explored both photometric colours and spectroscopic specific star formation rate from optical observations of galaxies, in a wide range of environments, in and near rich clusters in the local Universe, to examine cases where the usual correlation between the two fails to hold.

We find that >80% of the red galaxies ($(g-r)^{0.1} \geqslant 0.8$) that are classified to be part of the red sequence of clusters, on the basis of photometric colours, also have very little or no star formation (log SFR/M$^*\leqslant$-10.16 yr^{-1}, see Fig. 2). Similarly, 65% of the blue galaxies found within $3\,r_{200}$ of rich clusters also have high SSFR. However, in addition to these 'normal' galaxies in which the colour and spectroscopic SFR/M* correspond well with each other, a significant fraction of galaxies deviate from the norm, and would be classified differently, if treated solely on the basis of one of their spectroscopic and photometric properties.

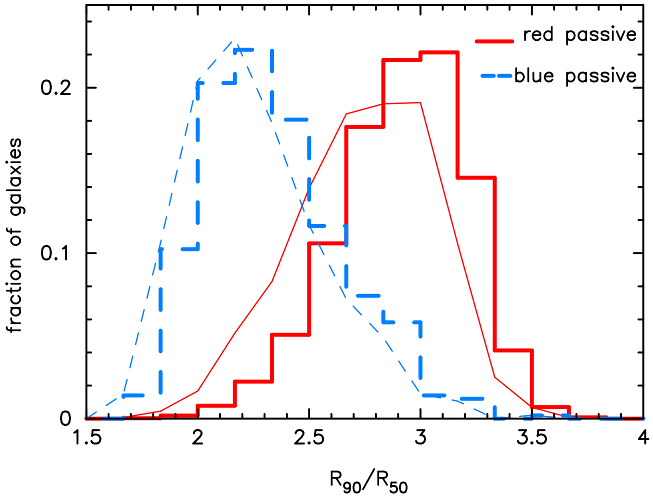

Figure 10. The distribution of the concentration parameter, C ≡ R_{90}/R_{50} for the red sequence (*red solid*) and blue passive (*blue dashed*) galaxies respectively. The thick and thin lines represent the distributions with and without unclassified galaxies in each case respectively. The blue passive galaxies clearly have late-type morphologies along with bluer colours. The fact that these galaxies have very low SSFR thus make them candidates for progenitors of the red sequence galaxies, in which star formation has been recently ($<$ 1 Gyr) truncated, eventually leading to red colour and early-type spheroidal structure typical of the present day cluster red-sequence galaxies.

4.1 Blue passive galaxies

The blue passive galaxies in our cluster sample (Fig. 2) have spectroscopic properties quite similar to their star-forming counterparts. The colour of a galaxy cannot be expected to, and indeed does not, correlate in the same way with environmental properties, as the star formation properties do (e.g., Kauffmann et al. 2003b). Our analysis shows that the values for the D_n4000 (Fig. 6) and internal extinction (A_z; Fig. 4) for blue passive galaxies are similar to those of blue star-forming galaxies, but the H_δ EW distribution (Fig. 5) is very different for the two populations. Since our sample is chosen to be in or near rich clusters, the discrepancy between their mean photometric colour, and their SSFR derived from spectra, suggests two possible scenarios: (i) these are galaxies in which star formation has been recently (∼1-2 Gyr) shut off due to the impact of local and/or global environment (e.g. Porter & Raychaudhury 2005, 2007; Porter et al. 2008; Mahajan, Raychaudhury & Pimbblet in preparation), or (ii) these are bulge dominated galaxies where the mean colour is dominated by the young stellar populations distributed in the disc but the spectrum sourced from an almost dead centre shows little sign of star formation activity.

A galaxy that has experienced a major burst of star formation 1-2 Gyr ago will show significant absorption in H_δ, which is found in a non-negligible fraction of the blue passive galaxies here (Figs. 5 and 7). This is because the A stars which significantly contribute to the H_δ absorption, have a lifetime of ∼1.5 Gyr, but the burst of star formation produces enough ionizing radiation to fill in the H_δ absorption line. But the absorption line shows up in the galaxy spectrum once the starburst has been truncated/ended.

Fig. 10 provides statistically significant evidence in favour of (ii). As a morphological index, here we use the concentration parameter $C \equiv R_{90}/R_{50}$, where R_x is the Petrosian radius encompassing x% of the galaxy's light in the r-band from SDSS images.

Table 2. K-S test results for distributions in Fig. 10 & 11 respectively

Distributions	D	p
Red & blue star-forming galaxies (including unclassified galaxies)	0.67	0.0000
Red & blue star-forming galaxies (excluding unclassified galaxies)	0.60	0.0000
Red star-forming galaxies (including & excluding unclassified galaxies)	0.08	0.1870
Blue star-forming galaxies (including & excluding unclassified galaxies)	0.02	0.9999
Red & blue passive galaxies (including unclassified galaxies)	0.35	0.0000
Red & blue passive galaxies (excluding unclassified galaxies)	0.29	0.0000
Red passive galaxies (including & excluding unclassified galaxies)	0.08	0.1772
Blue passive galaxies (including & excluding unclassified galaxies)	0.01	0.9999

In Fig. 10, we plot the distribution of C for the red and blue passive galaxies respectively. The blue passive galaxies clearly show late-type morphologies ($C < 2.6$; Strateva et al. 2001), while their red counterparts mostly have values of concentration typical of spheroidals. The galaxies in the former category are similar to the passive blue spirals that have been studied by other authors (e.g. Goto et al. 2003a; Wild et al. 2008).

By analysing the spatially resolved long-slit spectroscopy of a few passive spiral galaxies selected from the SDSS, Ishigaki et al. (2007) find that the H_δ absorption lines are more prominent in the outer regions of the disc, while the nuclear regions show strongest values for D_n4000. Their findings are consistent with the idea that the star formation in passive late-type galaxies ceased a few Gyr ago. Hence, the blue passive galaxies can be considered to be the progenitors of their red counterparts, in which star formation has been recently shut-off: these galaxies will eventually acquire redder colours and early-type morphologies, over a period that depends upon their environment (Goto et al. 2003c). Kannappan et al. (2009) have recently identified, characterized and studied the evolution of galaxies which, though morphologically classified as E/S0s, lie on the blue sequence in the colour-stellar mass space, and suggest that these systems almost always have a bluer outer disk, and that they are a population in transition, potentially evolving on to the red sequence, or have (re)formed a disk and are about to fall back in the class of late-types.

4.2 Red star-forming galaxies

Even more interesting are red galaxies with signs of active star formation in their fibre spectra. We find that 53.4% of the 539 galaxies in this class have significant emission lines on the basis of which their SSFR has been evaluated. These red star-forming galaxies are made up of at least two kinds of galaxies (chosen from simple limits in colour and SSFR). One kind appears to be very similar in photometric properties to the red sequence galaxies but with spectroscopically derived properties consistent with their late-type counterparts, while the other class has both photometric *and* spectroscopic properties similar to the red sequence galaxies, yet has a high SSFR.

The origin of the latter class is not clear. It is likely that these galaxies are currently experiencing a starburst, which has started very recently ($\lesssim$0.5 Gyr). Stellar populations resulting from such a starburst would be detected in spectral indices such as H_α EW (leading to high values of SFR/M*), but will not dominate the D_n4000 and the H_δ EW for another $\sim$0.5–1 Gyr. The former sub-population is most likely to be bright cluster galaxies (BCGs), with nuclear star-formation linked with the AGN (see Goto 2006; Bildfell et al. 2008; Reichard et al. 2009). In the following we turn our attention to this sub-population.

4.2.1 *Star formation at the core of giant ellipticals*

The hypothesis that AGN and star formation activity in the core of a galaxy may be linked is supported by the fact that $\sim$30% of the red star-forming galaxies with emission lines are classified as AGN on the BPT diagram. The fact that 50% of the emission-line red sequence galaxies (defined according to Fig. 2) are also classified as AGN does not contradict this scenario because either (i) the red sequence AGN galaxies in general have high stellar mass, and so can have low SSFR even though they have significantly high SFR, or (ii) they do not have enough cold gas to form stars, because of the presence of an active nuclei.

A significant fraction of giant ellipticals show evidence of on-going star formation or signs of recent (<2 Gyr) star formation in their cores, particularly in environments where the likelihood of recent mergers is high (e.g., McDermid et al. 2006; Nolan et al. 2006; Nolan, Raychaudhury, & Kabán 2007). For a sample of BCGs in 48 X-ray luminous clusters, Bildfell et al. (2008) find that 25% of the BCGs have colour profiles $(g-r)$ that turn bluer toward the centre. Our radial distribution of galaxies in this category (Fig. 3), compared to the distribution of blue star-forming galaxies, is consistent with this (see §2.5).

Elsewhere, Gallazzi et al. (2009) analyse an extensive dataset, covering UV to IR SEDs for galaxies in the Abell 901/902 cluster pair, to show that $\sim$40% of the star-forming galaxies residing in intermediate to high density environments have optically red colours. They show that these galaxies are not starbursts, and have SFRs similar to or lower than that of their blue counterparts. Whether the occurrence of blue cores in red sequence galaxies is linked to their nuclear activity, and whether the nuclear activity itself is modulated by the immediate environment of a galaxy (such as the presence of close neighbours), remains a debatable issue. We intend to return to this in future work involving a more detailed study of nuclear starbursts (also see Li et al. 2008; Reichard et al. 2009).

The scenario discussed in (ii) above complements the blue passive galaxy population discussed in §4.1– massive galaxies without much cold gas could be formed in dry major mergers of the passive blue progenitors, while high speed encounters amongst them in moderately dense environments, such as in the infall regions of clusters (e.g. Porter et al. 2008; Mahajan, Raychaudhury & Pimbblet in preparation), could lead to excessive loss of cold gas, leaving the galaxy to evolve passively thereafter.

In a spatially resolved spectroscopic study of 48 early-type galaxies, the SAURON team (de Zeeuw et al. 2002) simultaneously observed the CO(1-0) and CO(2-1) lines with 28% detection rate (12/43) (Combes et al. 2007). In this sample they find that the CO-rich galaxies show strongest evidence of star formation in the central ($\sim$4x4 arcsec^2) regions and also tend to have higher H_β and lower Fe5015 and Mg*b* indices. The results presented in this work also support various studies based on the UV data obtained by the Galaxy Evolution Explorer (*GALEX*) which suggests that a significant fraction ($\sim$15%) of bright ($M_r < -22$) early-type galaxies show signature of recent ($\lesssim$1 Gyr old) star formation (e.g.Yi et al. (2005); also see Crocker et al. (2009); Gallazzi et al. (2009)).

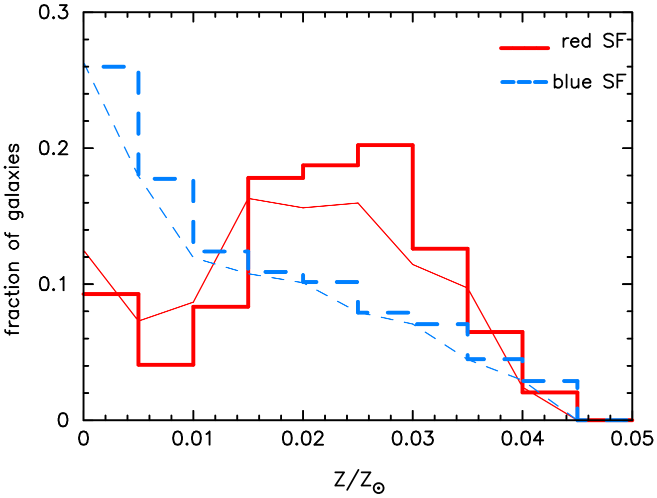

Figure 11. The distribution of stellar metallicities (from Gallazzi et al. 2005) for the red star-forming (*red solid*) and blue star-forming (*blue dashed*) cluster galaxies in our sample. The thick and thin curves are distributions including and excluding the unclassified galaxies respectively in each case. The distributions evidently show that the stars in the red star-forming galaxies are much more metal-rich with respect to their bluer counterparts. Given that the internal extinction in galaxies belonging to the two categories does not show a significant difference (Fig. 4), presence of metal-rich stellar populations in the red star-forming galaxies seems to be a likely cause of their redder colours.

4.2.2 *Stellar and gas phase metallicities*

Since star formation in a galaxy is often associated with the presence of dust, one would naively expect these red star-forming galaxies to be the dusty starburst galaxies widely discussed in the literature (Wolf, Gray & Meisenheimer 2005; Bildfell et al. 2008; Koyama et al. 2008; Saintonge, Tran & Holden 2008; Gallazzi et al. 2009; Wolf et al. 2009). However, we find that only $\sim$ 50% of the galaxies in this class show presence of any optical extinction (Figs. 4 & 9). So why are the rest of the galaxies red?

To address this question, we explore two other factors affecting galaxy colours, namely age and metallicity. We use stellar metallicities and mean luminosity-weighted stellar ages from the work of Gallazzi et al. (2005), which are estimated from 150,000 Monte Carlo simulations of a full range of physically plausible star formation histories. These models are logarithmically distributed in a metallicity range of 0.2–2.5 $Z_\odot$. In a given model, all stars have the same metallicity, interpreted as the 'luminosity-weighted stellar metallicity'. For each model in the library, Gallazzi et al. (2005) measure the strength of the D_n4000, and the H_β, $H_{\delta A}$+$H_{\gamma A}$, [Mg_2Fe] and [MgFe]$'$ spectral indices in the same way as they are measured in the SDSS spectrum of a galaxy. By comparing the strengths of these indices in the observed spectrum to the model spectra in their library, the probability density functions (PDFs) of several physical parameters, such as age and metallicity of a galaxy, are constructed.

We use the r-band luminosity weighted ages (hereafter referred to as 'mean galaxy ages') and stellar metallicities derived from these PDFs[2]. For galaxies in our cluster sample, we find that the red star-forming galaxies are systematically older than their blue counterparts by 5-7 Gyr. In Fig. 11, we compare the distributions of stellar metallicities of the red and blue star-forming galaxies. We confirm that the two distributions are statistically different by using the Kolmogorov-Smirnoff (K-S) statistics, which finds the probability of two datasets being drawn from the same parent population. The K-S test finds the maximum difference between the cumulative frequency distributions of the red and blue star-forming galaxies to be $D = 0.35$, with the probability of the null hypothesis being satisfied to be essentially zero.

Further support for the presence of excessive metals in the red star-forming galaxies is provided by a comparison between the gas-phase metallicities (log[O/H]+12) estimated by Tremonti et al. (2004)[3], who have compiled a sample of ∼53,000 star-forming galaxies from the entire SDSS DR4 (selected to have H_α, H_β & [NII] emission lines at $> 5\sigma$ detection). We find that the cumulative distributions of the gas-phase metallicities of the red and blue populations are statistically different. The K-S test yields $D = 0.18$ at a significance level of 0.043. Though the two samples compared here have widely different numbers of galaxies, our conclusion is consistent with that of Ellison et al. (2008), who show that for a sample of 43,690 galaxies, selected from the SDSS DR4, the gas-phase metallicities of galaxies with high SSFR are lower by 0.2 dex, compared to those with low SSFR at fixed stellar mass. The fact that their metallicities are estimated by a comparable but independent method (see Kewley & Dopita (2002) for details), further strengthens our result.

Around 35% of all red star-forming galaxies are classified as star-forming or composite galaxies from their spectra. This is in agreement with the results of Graves, Faber, & Schiavon (2009) who also find ∼30% of nearby red sequence galaxies from SDSS show presence of emission lines in their spectrum. They analyse LINER like emission in these galaxies to show that they are systematically younger by 2.5-3 Gyrs than their quiescent counterparts without emission at fixed rotational velocity. At $z \sim 0.1$, Tremonti et al. (2004) have shown that the metallicity is well correlated with the stellar mass of the galaxy. These quantities correlate well for $8.5 \leqslant \log M^* \leqslant 10.5\, M_\odot$, but the relation flattens thereafter. The fact that $\geqslant$60% of our red galaxies have log M^* in the range 10.6-10.9 $M_\odot$ supports the hypothesis that a significant fraction of the red star-forming galaxies obtain their red colours from the residual older generations of stars.

We have also shown that ∼50% of all the red star-forming galaxies are likely to be attenuated by >0.2 mag in the SDSS z-band (Fig. 4), and have bimodal H_δ EW and D_n4000 distributions (Figs. 5, 6 and 7) which are very different from that of the typical red sequence galaxies. As discussed in §3.1 and §3.2, the red star-forming class of galaxies remain bimodal in the distributions of A_z, H_δ and D_n4000, even if the selection criterion based on SFR/M^* is changed to a significantly different value (e.g. ∼15-percentile, corresponding to log SFR/M^* = -10 yr^{-1}). This clearly indicates that the component of red star-forming galaxies that are similar in properties to the red sequence galaxies are not merely a result of scatter from the red sequence (quadrant 1; Fig. 2).

4.3 Implications for the Butcher-Oemler effect

Butcher & Oemler (1984) found that clusters at moderate to high redshift contain an excess of blue galaxies, compared to their low-redshift counterparts. For the redshift regime of our sample ($z \sim 0.1$), they found a uniform blue fraction f_b of ∼0.03 in all clusters within R_{30}, the radius containing 30% of the cluster's red sequence population. This exercise has been repeated several times in recent years for many samples of clusters (Butcher & Oemler 1984; Margoniner & Carvalho 2000; Ellingson et al. 2001; De Propris et al. 2004). Most studies of this kind define 'blue' galaxies in terms of a broadband colour that is bluer by 0.2 mag than that of the cluster's red sequence galaxies. From the above discussion, it is clear that this cut leaves out a significant fraction of star-forming galaxies that have redder broadband colours, and classifies some passively evolving galaxies as 'star-forming'.

Margoniner & Carvalho (2000) found the blue fraction of galaxies to be f_b=0.03±0.09, similar to Butcher & Oemler (1984), for 44 Abell clusters at $0.03 \leqslant z \leqslant 0.38$ within a fixed cluster-centric distance of 0.7 Mpc, which translates into the mean R_{30} for most Abell clusters below $z \lesssim 0.1$. However, Margoniner et al. (2001) measured the fraction to be $(1.24 \pm 0.07)z - 0.01$ for clusters at $z \leqslant 0.25$, again for galaxies within a fixed cluster-centric aperture of 0.7 Mpc. Elsewhere (Ellingson et al. 2001; De Propris et al. 2004), various multiples of cluster-centric radius, scaled with r_{200}, have been used to show the effect of chosen aperture size on the blue fraction. Ellingson et al. (2001) suggest that the origin of the Butcher-Oemler effect lies in the fact that the relative fraction of 'blue' galaxies on the outskirts of the clusters at higher redshifts is higher than in their local counterparts. If confirmed, this result can have a critical impact on the study of evolution of galaxy properties. It is worth mentioning here that even though most of these studies use optical spectra for most or all of their sample (except for Butcher & Oemler (1984)), the spectroscopic information is used only for assigning cluster membership.

Recently, with the increasing availability of large multi-wavelength datasets, the possibility of the Butcher-Oemler effect being observed in other fundamental galaxy properties (e.g. morphology, Goto et al. 2003b), or in non-optical data (e.g. mid-IR, Saintonge, Tran & Holden 2008), is being explored. The study of Wolf, Gray & Meisenheimer (2005) unraveled the presence of young stars and dust in the red sequence galaxies in a cluster pair at z∼0.17, while Bildfell et al. (2008) find that the colour profile of 25% of the brightest cluster galaxies (BCGs) turn bluer by 0.5–1.0 mag towards their centres, compared to the average colours seen in the cluster's red sequence. All of this has serious implications for Butcher-Oemler like effects based on global photometric properties.

Our sample provides some additional insight to this discussion. The presence of metals, and of colour gradients related to SFR in a galaxy, will affect the estimated fraction of 'star-forming' galaxies in low redshift clusters. The fact that nearby cluster galaxies are more metal-rich than those in high-redshift clusters, will artificially enhance the fraction of passive galaxies that are selected solely on the basis of their colour. Such an effect is usually not accounted for while comparing the blue/star-forming galaxy fraction in clusters at different redshifts. A quantitative analysis of this effect requires a consistent study of an unbiased sample of mutually comparable galaxy clusters spanning a wide redshift range, for which both photometric and spectroscopic multi-wavelength data is available. We leave this for a later consideration.

---

[2] http://www.mpa-garching.mpg.de/SDSS/DR4/Data/stellarmet.html

[3] http://www.mpa-garching.mpg.de/SDSS/DR4/Data/oh_catalogue.html

5 SUMMARY AND CONCLUSION

We divide a sample of $>$6,000 galaxies found in or near rich Abell clusters (z$\leqslant$0.12) in the SDSS spectroscopic catalogue, into four populations, defined by placing simple limits in $(g-r)^{0.1}$ colour (derived from photometry) and specific star formation rate (derived from the detailed modelling of optical spectra). While most blue galaxies have evidence of star formation, and red galaxies do not, this identifies two significant populations of blue passive galaxies and red star-forming galaxies.

We trace the spectroscopic and photometric properties of galaxies in these four sub-samples in detail, using data available from SDSS DR4. The main results of our analysis can be summarised as follows:

- For the blue passive galaxies, the dust content and values for the D$_n$4000 are similar to those of the blue star-forming galaxies, indicating similar metal content, mean ages and internal extinction.
- Since the blue passive galaxies have a broad distribution of H$_\delta$ EW, along with late-type morphologies, they appear to be similar to the passive blue spirals studied by other authors. Our results support the hypothesis that these galaxies could be the progenitors of the red sequence galaxies in which star formation has been recently shut off due to the impact of local/global environment.
- An intriguing find of this study is that only $\sim$50% of the red star-forming galaxies have significant values of extinction, indicative of the presence of dust.
- By comparing the stellar metallicities, gas-phase metallicities and mean ages of the red and blue star-forming galaxies, we find statistically significant evidence in support of the fact that, for at least half of the red star-forming galaxies, the red colours result from a relatively metal-rich stellar population. Our argument remains valid even if the criterion for classification as star-forming based on SSFR is changed within reasonable limits (15-50 percentile, instead of the 25-percentile used in this work).
- A significant ($\sim$15%) fraction of the red star-forming galaxies have blue cores, indicating recent star formation which might be linked to the AGN activity in these galaxies.
- The population of passive red sequence galaxies increase toward the cluster centre, closely followed by the red star-forming galaxies, except that the latter does not rise steeply in the cluster core.
- The blue star-forming galaxies are distributed uniformly at 1-3r$_{200}$ from the cluster centre, but decline steeply within r$_{200}$. The blue passive galaxies on the other hand show a constant distribution, except for a small increase around 2r$_{200}$.
- Galaxy evolution studies which base their sample selection criterion only on broadband colours to test Butcher-Oemler like effects, may be significantly affected by the presence of ‘complex’ galaxy populations such as the red star-forming and blue passive galaxies discussed here.

6 ACKNOWLEDGMENTS

Funding for the Sloan Digital Sky Survey (SDSS) has been provided by the Alfred P. Sloan Foundation, the Participating Institutions, the National Aeronautics and Space Administration, the National Science Foundation, the U.S. Department of Energy, the Japanese Monbukagakusho, and the Max Planck Society. The SDSS Web site is http://www.sdss.org/. This research has made use of the SAO/NASA Astrophysics Data System. SM is supported by grants from ORSAS, UK, and the University of Birmingham.

We are very thankful to the anonymous referee for the constructive comments and a comprehensive review of the paper.

REFERENCES

Abell G.O., Corwin H.G., Jr., Olowin R.P., 1989, ApJS, 70, 1
Adelman-McCarthy J.K., et al., 2006, AJS, 162, 38
Ann H. B., Park C., Choi Y.-Y., 2008, MNRAS, 389, 86
Ashman K.M., Bird C.M., Zepf S.E., 1994, AJ, 108, 2348
Baldwin J.A., Phillips M.M., Terlevich R., 1981, PASP, 93, 5
Balogh M.L., Morris S.L., Yee H.K.C., Carlberg R.G., Ellingson E., 1999, ApJ, 527, 54
Balogh M.L., Baldry I K., Nichol R., Miller C., Bower R., Glazebrook K., 2004a, ApJ, 615L, 101B
Balogh M.L., et al., 2004b, MNRAS, 348, 1355
Beers T.C., Flynn K., & Gebhardt K., 1990, ApJ, 100, 32
Best P.N., Kauffmann G., Heckman T.M., Brinchmann J., Charlot S., Ivezic’ $\check{Z}$., White S.D.M., 2005, MNRAS, 362, 25B
Bildfell C., Hoekstra H., Babul A., Mahdavi A., 2008, MNRAS, 389, 1637
Blanton M.R., et al., ApJ, 129, 2562
Brinchmann J., Charlot S., White S.D.M., Tremonti C., Kauffmann G., Heckman T., Brinkmann J., 2004, MNRAS, 351, 1151
Bruzual A.G., 1983, ApJ, 273, 105
Bruzual A.G., Charlot S., 1993, ApJ, 405, 538
Butcher H., Oemler A., Jr., 1984, ApJ, 285, 426
Calzetti D., 1994, ApJ, 429, 582C
Calzetti D., 1997, AJ, 113, 162
Cao C., Wu H., Wang J., Hao C., Deng Z., Xia X., Zou Z., 2006, ChJAA, 6, 197
Carlberg R.G., Yee H.K.C., Ellingson E., 1997, ApJ, 478, 462
Charlot S., Fall S.M., 2000, ApJ, 539, 718
Charlot S., Longhetti, M., 2001, MNRAS, 323, 887
Cooper M.C., et al., 2007, MNRAS, 376, 1445
Combes F., Young L.M., Bureau M., 2007, MNRAS, 377, 1795
Crocker A.F., Jeong H., Komugi S., Combes F., Bureau M., Young L.M., Yi S., 2009, MNRAS, 393, 1255
De Propris R., et al., MNRAS, 2004, 351, 125
de Zeeuw P.T., et al., 2002, MNRAS, 329, 513
Diaferio A., Geller M. J., 1997, ApJ, 481, 633
Dressler A., 1980, ApJ, 236, 531
Dünner R., Reisenegger A., Meza A., Araya P. A., Quintana H., 2007, MNRAS, 376, 1577
Ellingson E., Lin H., Yee H.K.C., Carlberg R.G., 2001, ApJ, 547, 609
Ellison S.L., Patton D.R., Simard L., McConnachie A.W., 2008, ApJ, 672, L107
Faber S.M., 1973, ApJ, 179, 731
Gallazzi A., Charlot S., Brinchmann J., White S.D.M., Tremonti C.A., 2005, MNRAS, 362, 41
Gallazzi A., et al., 2009, ApJ, 690, 1883G
Giovanelli R., Haynes M. P., 1985, ApJ, 292, 404
Gòmez P.L., et al., 2003, ApJ, 584, 210
Goto T., et al., 2003a, PASJ, 55, 771
Goto T., et al., 2003b, PASJ, 55, 739
Goto T., et al.,2003c, PASJ, 55, 757G
Goto T., 2006, MNRAS, 369, 1765
Graves G.J., Faber S.M., Schiavon R.P., Yan R., 2007, ApJ, 671, 243
Graves G.J., Faber S.M., Schiavon R.P., 2009, ApJ, 693, 486

Haines C.P., La Barbera F., Mercurio A., Merluzzi P., Busarello G., 2006a, ApJ, 647L, 21H

Haines C.P., Merluzzi P., Mercurio A., Gargiulo A., Krusanova N., Busarello G., La Barbera F., Capaccioli M., 2006b, MNRAS, 371, 55

Haines C.P., Gargiulo, A., La Barbera F., Mercurio A., Merluzzi P., Busarello G., 2007, MNRAS, 381, 7

Haines C.P., Gargiulo A., Merluzzi P., 2008, MNRAS, 385, 1201

Ishigaki M., Goto T., Matsuhara H., 2007, MNRAS, 382, 270

Kannappan S.J., Guie J.M., Baker A.J., 2009, AJ, 138, 579K

Kauffmann G., et al., 2003a, MNRAS, 341, 33

Kauffmann G., et al., 2003b, MNRAS, 341, 54

Kauffmann G., et al., 2003c, MNRAS, 346, 1055

Kewley L.J., Heisler C.A.,

Kewley L.J., Dopita M.A., 2002, ApJS, 142, 35

Khosroshahi H. G., Raychaudhury S., Ponman T. J., Miles T. A., Forbes D. A., 2004, MNRAS, 349, 527

Koyama Y., et al., 2008, MNRAS, 391, 1758

Lewis I., et al., 2002, MNRAS, 334, 673L

Li C., Kauffmann G., Heckman T.M., White S.D.M., Jing Y.P., 2008, MNRAS, 385, 1915

Lupton R., Gunn J.E., Ivezic Z., et al. 2001, in Astronomical Data Analysis Software and Systems X, ed. F.R. Harnden, Jr., F.A. Primini, H.E. Payne (San Francisco: ASP), ASP Conf. Ser., 238, 269

Mahajan S., Raychaudhury S., Pimbblet K., 2009, in preparation

Margoniner V.E., de Carvalho R.R., 2000, AJ, 119, 1562

Margoniner V.E., de Carvalho R.R., Gal R.R., & Djorgovski S.G., 2001, ApJ, 548, L143

Melnick J., Sargent W.L.W., 1977, ApJ, 215, 401

McDermid R. M., et al., 2006, MNRAS, 373, 906

Miles T. A., Raychaudhury S., Russell P. A., 2006, MNRAS, 373, 1461

Noeske K.G., Faber S.M., Weiner B.J., et al., 2007, MNRAS, ApJ, 660L, 47

Nolan L. A., Raychaudhury S., Kabán A., 2007, MNRAS, 375, 381

Nolan L. A., Harva M. O., Kabán A., Raychaudhury S., 2006, MNRAS, 366, 321

Oemler A.J., 1974, ApJ, 194, 1

Oemler A., Dressler A., Kelson D., Rigby J., Poggianti B. M., Fritz J., Morrison G., Smail I., 2009, ApJ, 693, 152

Osterbrock D.E., 1989, Astrophysics of Gaseous Nebulae and Active Galactic Nuclei (Mill Valley: University Science Books)

Pimbblet K.A., Smail A., Edge A.C., O'Hely E., Couch W.J., Zabludoff A.I., 2006, MNRAS 366, 645

Porter S. C., Raychaudhury S., 2005, MNRAS, 364, 1387

Porter S.C., Raychaudhury S., 2007, MNRAS, 375, 1409

Porter S.C., Raychaudhury S., Pimbblet K.A., Drinkwater M.J., 2008, MNRAS, 388, 1152

Prochaska L.C., Rose J.A., Caldwell N., Castilho B.V., Concannon K., Harding P., Morrison H., Schiavon R.P., 2007, AJ, 134, 321

Raychaudhury S., von Braun K., Bernstein G. M., Guhathakurta P., 1997, AJ, 113, 2046

Reichard T.A., Heckman T.M., Rudnick G., Brinchmann J., Kauffmann G., Wild V., 2009, ApJ, 691, 1005

Rines K., Diaferio A., 2006, AJ, 132, 1275

Rines K., Geller M.J., Kurtz M.J., Diaferio A., 2003, AJ, 126, 2152

Saintonge A., Tran K.H., Holden, B.P., 2008, ApJ, 685, L113

Strateva,I., et al., 2001, AJ, 122, 1861

Trager S.C., Faber S.M., Worthey G., Gonzalez J.J., 2000, AJ, 119, 1645

Tremonti C., et al., 2004, ApJ, 613, 898

Weinmann S.M., van den Bosch F.C., Yang X., Mo H.J., 2006, MNRAS, 366, 2

Wild V., Walcher C.J., Johansson P.H., Tresse L., Charlot S., Pollo A., Le Fevre O., de Ravel L., 2009, MNRAS, 395, 144W

Worthey G., Ottaviani D.L., 1997, ApJS, 111, 377

Wolf C., Gray M.E., Meisenheimer K., 2005, A&A, 443, 435

Wolf C., et al., 2009, MNRAS, 393, 1302W

Yang X., Mo H.J., Van den Bosch F.C., Pasquali A., Li C., Barden M., 2007, ApJ, 671, 153

Yi S.K., et al., 2005, ApJ, 619, L111